

PAPER

Comparative Biomechanical Evaluation of Unilateral and Bilateral Cages in Posterior Lumbar Interbody Fusion: Endplates Subsidence, Pedicle Screw Loosening and Implant Stability

Nur Saliha Md Salleh,
Muhammad Hazli
Mazlan(✉), Muhammad
Anas Razali

Faculty of Electrical and
Electronic Engineering,
Universiti Tun Hussein Onn
Malaysia, Johor, Malaysia

mhazli@uthm.edu.my

ABSTRACT

Implant sinking, pedicle screw loosening, and instability are commonly observed complications in posterior lumbar interbody fusion (PLIF) surgeries, attributed to a range of mechanical, biomechanical, and environmental factors. To address these challenges, the utilization of unilateral cages positioned obliquely, along with bilateral posterior instrumentation, and employing a material with a comparable modulus to cortical bone, has shown promising efficacy. The present study employed image-based finite element analysis (FEA) to evaluate the influences on cage sinking, screw loosening, and construct stability. The outcomes revealed that obliquely positioned unilateral fusion cage constructs with posterior instrumentation yielded superior biomechanical outcomes, characterized by reduced range of motion and stress distortion at the cage-endplate and screw-bone junctions. Furthermore, these findings indicated a lower risk of fractures and diminished deformations in normal and traumatic events. Hence, the utilization of biocompatible cage materials and structural symmetry holds critical significance for achieving biomechanical success in PLIF surgery.

KEYWORDS

unilateral and bilateral cages, posterior lumbar Interbody fusion, fracture risks assessment

1 INTRODUCTION

PLIF with accompanying posterior instrumentation (PI) is a surgical intervention designed to address severe back pain, promote spinal stability, and facilitate fusion [1]. It is typically employed in cases characterized by severe degenerative disc disease and disc space collapse. Furthermore, spinal fusion may be warranted in various other conditions, such as spinal disc herniation, vertebral fractures, scoliosis, spondylosis,

Md Salleh, N.S., Mazlan, M.H., Razali, M.A. (2023). Comparative Biomechanical Evaluation of Unilateral and Bilateral Cages in Posterior Lumbar Interbody Fusion: Endplates Subsidence, Pedicle Screw Loosening and Implant Stability. *International Journal of Online and Biomedical Engineering (iJOE)*, 19(18), pp. 123–138. <https://doi.org/10.3991/ijoe.v19i18.43833>

Article submitted 2023-08-09. Revision uploaded 2023-10-16. Final acceptance 2023-10-16.

© 2023 by the authors of this article. Published under CC-BY.

and kyphosis. This treatment has been widely accepted and has a good record of success, with 80,000 successful interbody fusions implanted between 1995 and 1999 [2].

Initially, medical-grade stainless steel or titanium alloys were used as the material for the cage in PLIF surgery. However, current exploration in medical research has led to the use of polyetheretherketone (PEEK), which has superior radiolucency and biocompatibility and has a Young's modulus nearer to cortical bone [3]. Although carbon fiber reinforced polymer (CF-P) has been considered for use, PEEK remains the favored choice due to its better elastic modulus. Previous research studies [4–7] have provided evidence to support the benefits of using PEEK cages in spinal surgeries. These studies have reported improved fusion rates ranging from 93% to 100% after a 12-month follow-up period. Additionally, PEEK cages have reduced subsidence rates at the cage-endplate interfaces, with reported rates ranging from 0% to 14.2%. Moreover, the clinical outcomes associated with PEEK cages have been consistently excellent, with reported success rates ranging from 80% to 96%.

The utilization of bilateral cages with PI offers an optimal solution for achieving high segmental stability. However, this approach entails increased risks and costs. Specifically, the insertion of a single spacer can cost between \$2,000 and \$5,000, while the use of bilateral cages necessitates broader adjustment of facetectomy and laminectomy, which elevates the incidence of nerve injury [8]. Considering these factors, cost-effectiveness, risk mitigation, and speedy recovery are crucial considerations for individuals pursuing spinal surgery. Consequently, there is a growing trend of requesting unilateral cages procedures. Obliquely oriented unilateral cages have been reported to have comparable potential to bilateral ones. Moreover, this configuration can significantly decrease stress at the cage-endplate interface, enhance stability, and reduce pedicle screw stress [9–11]. In an effort to further lessen the treatment costs, there have been attempts to implement unilateral pedicle screw and rod constructs. Nevertheless, this endeavor proves insufficient as it compromises construct stability, leading to screw loosening or construct failure under repetitive loads [9].

This research aims to evaluate the performance of using a unilateral PEEK cage integrated with bilateral PI, positioned obliquely, by comparing their biomechanical effectiveness with other cage constructs of the posterior lumbar interbody fusion (PLIF) procedure. The four cage constructs include bilateral PEEK, bilateral titanium, unilateral PEEK in an oblique orientation and unilateral titanium in an oblique orientation. The biomechanical analysis was conducted using finite element analysis (FEA) to examine parameters such as cage subsidence, construct stability, and loosening effect at the pedicle screw attachment area by analyzing maximal stress distribution and predicting fracture risk patterns. The research hypothesis suggests that the obliquely-placed unilateral PEEK cage will enhance segmental stability by effectively distributing a greater load through the cage and reducing stress on the pedicle screw-bone and cage-endplate junctions.

2 MATERIALS AND METHODS

2.1 Finite element (FE) modeling

The MECHANICAL FINDER software was used to create a 3D finite element model of the L4–L5 lumbar section. A healthy 29-year-old man patient's CT scans were used to build the model. The client weighed 78 kg, measured 176 cm in height, and had no previous medical history. The individual provided written informed consent before agreeing to participate in the study. Sagittal two-dimensional tomographic images of the T11–L5 vertebral body were acquired using a 128-row, 256-slice GE spiral CT scanner

(Sensation 16 Siemens, Germany). These scans were performed with a 1 mm slice thickness and a resolution of 512×512 , and the resulting data were saved in DICOM format.

The vertebral bodies were modeled as cancellous bone cores around 0.4 mm thick cortical shells in the 3D finite element model. 1.0 mm solid tetrahedral components were used to separate the facet joint cartilages, intervertebral discs, and cancellous bone. On the other hand, 1.0 mm linear shell triangle components were used to discretize the cortical bone. A mesh convergence study was conducted to determine the optimal mesh size for optimizing the FEA results. The convergence study involved selecting different mesh sizes of tetrahedral elements, applying simple FEA, and analyzing the results. In this study, seven mesh sizes ranging from 0.7 to 1.3 mm were applied, with a 1 kN distributed load applied to the top of L4. The bone displacement and maximum stress generated were then analyzed. The results indicated that the 1 mm mesh size exhibited a converged value for both bone displacement and maximum stress under the given load.

The methodology described by Keyak et al. [12] was used to compute Young's modulus and yield strength of each element according to the Hounsfield Unit (HU) values extracted from the CT scan images. The material properties of the bone were classified as non-linear and inhomogeneous. The bone material's Poisson ratio was fixed at 0.4 [12]. The cartilages of facet joints and intervertebral discs were modeled as linear, homogeneous materials. The intervertebral disc's Young's modulus (E) and Poisson's ratio were set at 8.4 MPa and 0.45, respectively, whereas the facet joint's values were 11 MPa and 0.2, respectively [13,14]. A fully bonded interface condition was included to ensure their relative motion was restrained within the vertebral bodies to imitate the confined movements between the facet joint cartilages and intervertebral disc cartilages.

Two interbody fusion implants were designed in computer-aided design (CAD) software. The first implant was set with titanium material, while another implant was set with PEEK material. The dimensions of the titanium implant were 22 mm in length, 10 mm in height, and 10 mm in width, while the PEEK implant had dimensions of 26 mm in length, 8 mm in height, and 10 mm in width. The cages were fixed into the intervertebral disc space between L4 and L5. The cages were symmetrically located around the midsagittal plane for bilateral cage fusion. For the unilateral cage fusion, the cage was positioned obliquely. A bilateral PI was implanted in the model. This involved the insertion of rods and pedicle screws and rods into the model. The PI was assigned titanium material. The contact surfaces of the PI were assumed to be perfectly bonded to ensure there was no sliding or separation at these interfaces.

Four PLIF constructs were developed, each featuring a different cage orientation, as illustrated in Figure 1. The models were subjected to compression (1000 N), flexion (4.2 Nm), extension (1.0 Nm), axial rotation (3.4 Nm) and lateral bending (2.6 Nm) loads [15]. These loads were subjected to the intervertebral disc immediately above the L4 vertebra, with 85% of the load directed to the intervertebral disc and the remaining load directed to the superior facet joint cartilages of L4. This setup followed the three-column load-bearing concept [16]. The bottom part of the model was fixed in all directions.

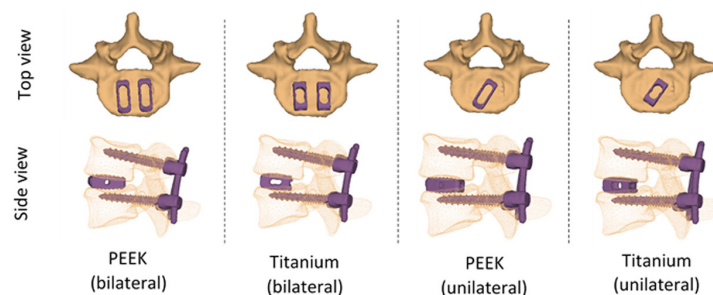


Fig. 1. Simulated PLIF constructs

2.2 Fracture analysis

Cage subsidence and pedicle loosening phenomena were carefully investigated by adopting non-linear FEA based on the Newton-Raphson method. Ten iterations of 1 kN load increments were applied to the models in order to replicate traumatic loading conditions. It has been reported that the ultimate compressive strength of the vertebral body is 8000 N [17], and the maximum 10 kN load is supposed to cause a 50% risk of injury [18]. The material properties for each element were assumed to be bi-linear elastoplastic, where the modulus of elasticity of the material was reduced to 95% of its initial value in a yielded state [19]. The behavior of the materials was isotropic, acting differently in tensile and compressive directions. The ultimate tensile stress was set at 80% of the compressive yield stress, and the crushing strain was fixed at $-10,000$ microstrains [20]. The workflows of the non-linear fracture risks prediction are described in Figure 2 [14,20]. The consideration of cage subsidence becomes relevant when one of the shell elements fails in a manner that could result in a significant clinical fracture. Thus, failure of a small portion of cancellous bone is considered insignificant as long as the cortical bone remains intact [20].

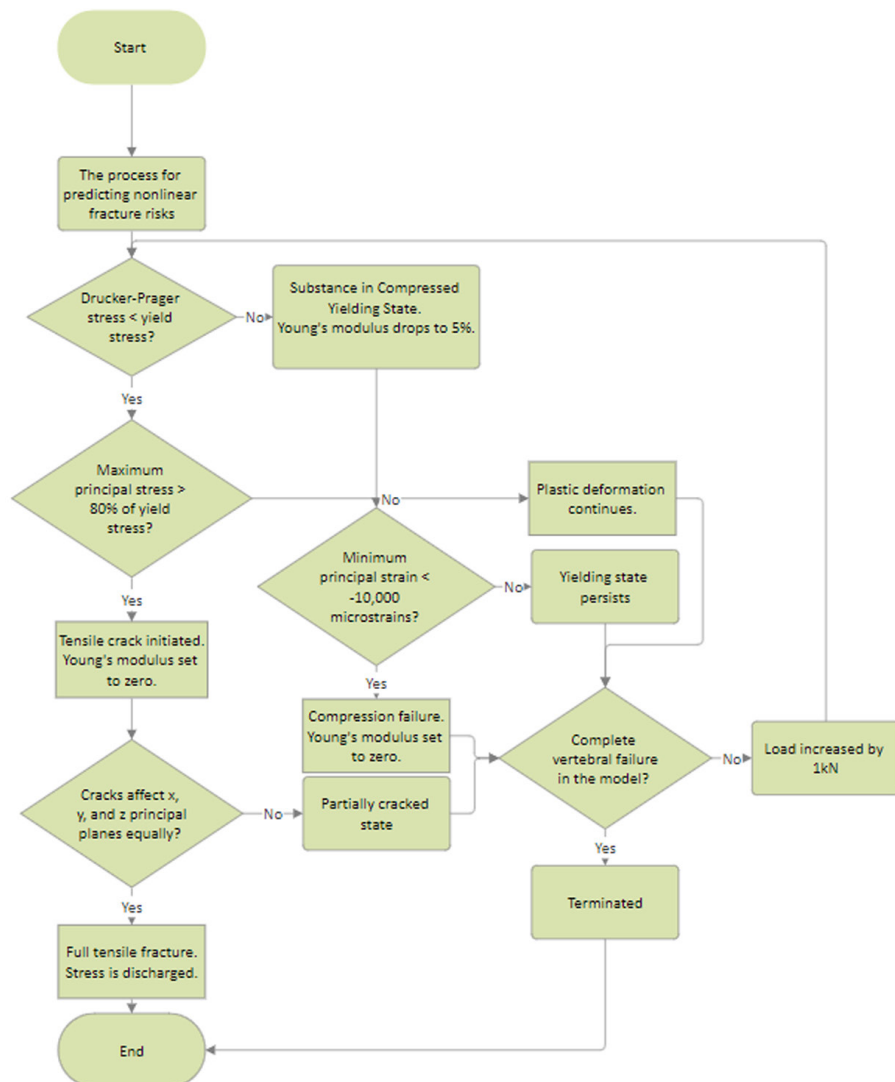


Fig. 2. The flowchart of failure elements determination

2.3 Relative movement of vertebrae

The range of motion (ROM) for each model was measured by computing the relative position of L4 in relation to L5 [21]. This was done by using perpendicular lines on the upper surface of each vertebra, associated with four knots, as shown in Figure 3.

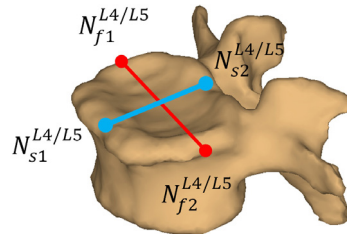


Fig. 3. Reference coordinates and lines in measuring the ROM of the vertebral models

The reference coordinates for every vertebra are divided into frontal and sagittal planes:

Frontal plane:

$$N_{f1}^{L4/L5} = N_{f1} (X_{f1} Y_{f1} Z_{f1}) \tag{1}$$

$$N_{f2}^{L4/L5} = N_{f2} (X_{f2} Y_{f2} Z_{f2}) \tag{2}$$

Sagittal plane:

$$N_{s1}^{L4/L5} = N_{s1} (X_{s1} Y_{s1} Z_{s1}) \tag{3}$$

$$N_{s2}^{L4/L5} = N_{s2} (X_{s2} Y_{s2} Z_{s2}) \tag{4}$$

The lengths of both lines were obtained using the formulae of analytical geometry as follows:

Frontal plane:

$$L_f = \sqrt{(X_{f2} - X_{f1})^2 + (Y_{f2} - Y_{f1})^2 + (Z_{f2} - Z_{f1})^2} \tag{5}$$

Sagittal plane:

$$L_s = \sqrt{(X_{s2} - X_{s1})^2 + (Y_{s2} - Y_{s1})^2 + (Z_{s2} - Z_{s1})^2} \tag{6}$$

Then the directional cosines are computed as follows:

Frontal plane:

$$l_f = \frac{X_{f2} - X_{f1}}{L_f}, m_f = \frac{Y_{f2} - Y_{f1}}{L_f}, n_f = \frac{Z_{f2} - Z_{f1}}{L_f}, \tag{7}$$

$$l_s = \frac{X_{s2} - X_{s1}}{L_s}, m_s = \frac{Y_{s2} - Y_{s1}}{L_s}, n_s = \frac{Z_{s2} - Z_{s1}}{L_s}, \tag{8}$$

Finally, the relative angles with respect to L5 in their respective spinal motions were computed via scalar product as follows:

Flexion, extension and compression:

$$\cos \alpha_{FE} (L_4 - L_5) = m_s^{L4} m_s^{L5} + n_s^{L4} \tag{9}$$

Lateral bending:

$$\cos \alpha_{LB}(L_4 - L_5) = l_f^{L4} l_f^{L5} + n_f^{L4} n_f^{L5} \tag{10}$$

Axial Rotation:

$$\cos \alpha_{AR}(L_4 - L_5) = l_f^{L4} l_f^{L5} + m_f^{L4} m_f^{L5} \tag{11}$$

Technically, the calculation of the range of motion (ROM) of the vertebrae has a direct relationship to the stability of the reconstructive configuration of the vertebrae. Thus, it is necessary to compare the stability of each vertebra model by evaluating their micro-motion activity.

3 RESULTS

3.1 Stress profiles

Cage-endplate interface stress. Figure 4 shows Drucker-Prager stress distributions of the various PLIF configurations under physiological spine motions. Twenty areas of interest (AOI) were chosen to scrutinize the stress distributions in the model. The stress distributions and the technique to obtain the AOI are shown in Figures 5 and 6, respectively. The results have shown that the obliquely positioned unilateral titanium cage construct exhibited the highest Drucker-Prager stresses for most spine motions. On the other hand, the obliquely placed unilateral PEEK generated the lowest Drucker-Prager stresses. It is worth noting that similar stress profiles were observed across all motion activities.

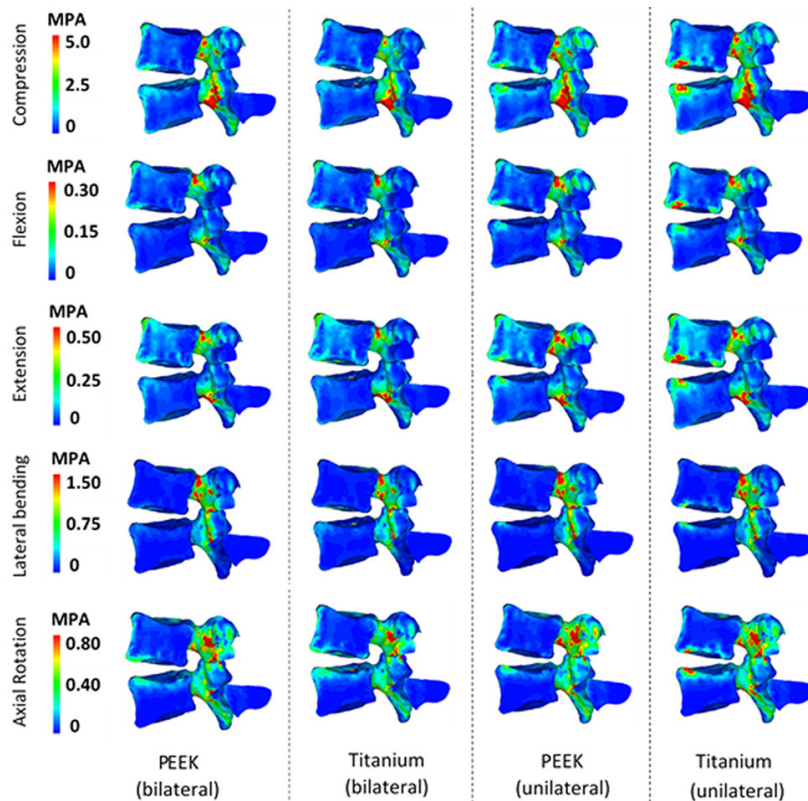


Fig. 4. Drucker-Prager stress distributions (sagittal views)

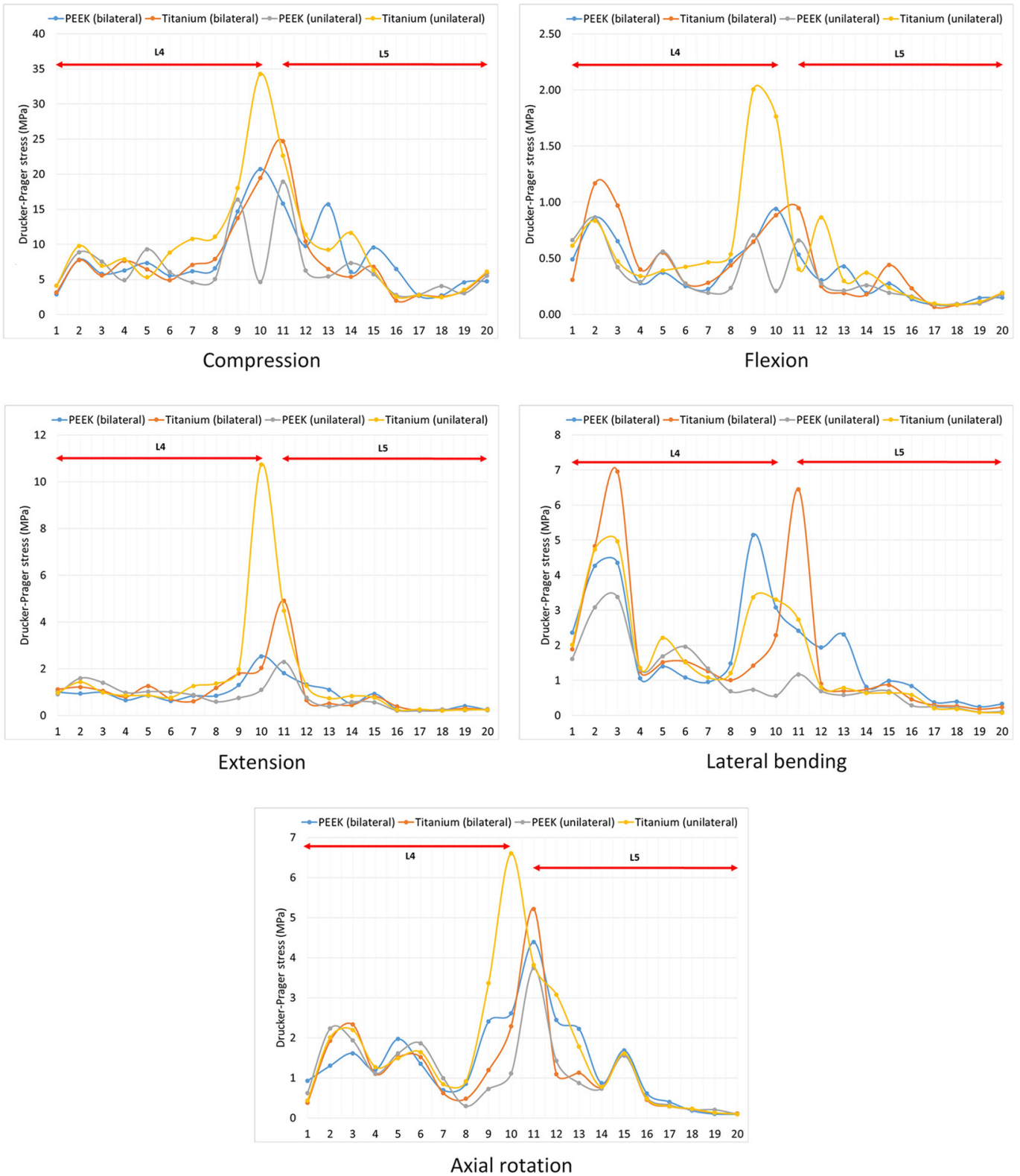


Fig. 5. Maximum Drucker-Prager stress distributions

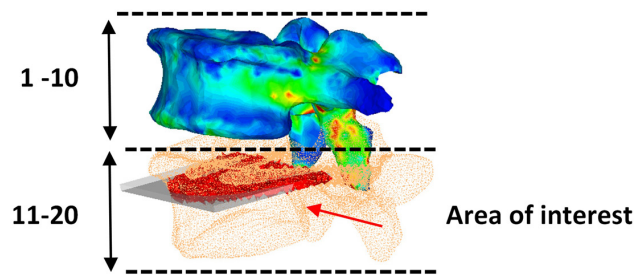


Fig. 6. Selection of twenty Aol to measure the maximum Drucker-Prager stress

The analysis reveals that the cage-endplate interface junctions experienced the highest stress generation in nearly all specified spine motions. This stress concentration, termed distortion stress, is likely a result of the stiffness mismatch between the vertebral bone and the cage. Figure 7 presents a bar graph summarizing the maximum Drucker-Prager stress distributions at the cage-endplate junction. The distortion stresses ranged from 1.12 MPa to 20.73 MPa for the bilateral PEEK cage, 1.00 MPa to 24.67 MPa for the bilateral titanium cage, 0.73 MPa to 18.9 MPa for the obliquely-placed unilateral PEEK cage, and 2.01 MPa to 38.19 MPa for the obliquely-placed unilateral titanium cage. Therefore, the obliquely-placed unilateral titanium cage exhibited the highest susceptibility to cage subsidence, followed by the bilateral titanium, bilateral PEEK, and obliquely-placed unilateral PEEK cages.

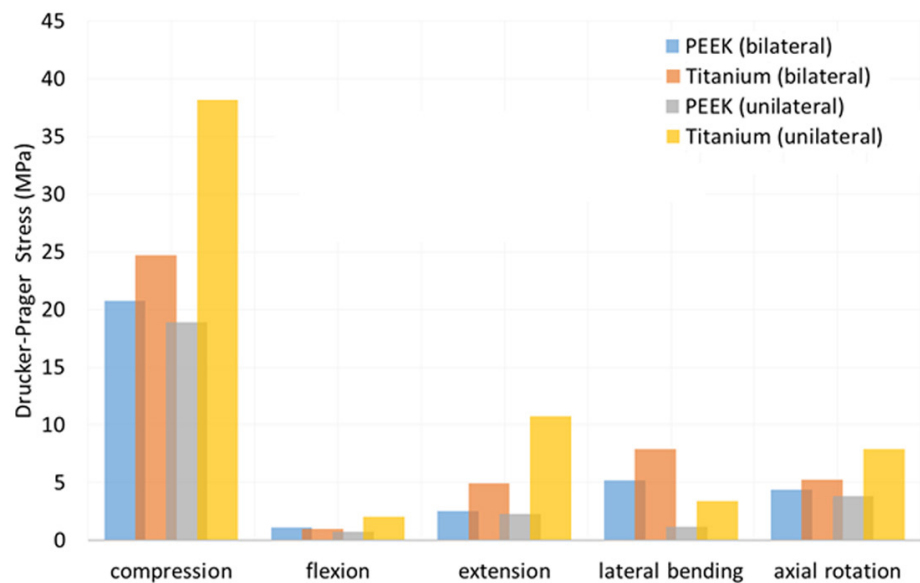


Fig. 7. Cage-endplate interface stress

The study findings suggest that the choice of cage material plays a vital role in mitigating the impact of cage subsidence, outweighing the influence of cage orientation. Specifically, it is concluded that using a cage material with properties closely resembling cortical bone yields the best results when employing an obliquely-placed cage. On the other hand, for stiffer materials, the bilateral cage configuration is considered the most practical approach. Therefore, while cage material is the key factor in addressing cage subsidence, the optimal cage orientation depends on the material properties used.

Bone-pedicle screw interface stress. The study extensively examined the impact of pedicle screw loosening by analyzing the maximal stresses at the bone-pedicle

screw interface, as illustrated in Figure 8. It is evident that the most significant variations in load-bearing occurred during compression activity. For all other motions, the responses of each configuration were nearly identical, with relative differences and maximal values being less than 10% and 10 MPa, respectively. Therefore, it was observed that the obliquely-placed unilateral titanium cage exhibited the highest inclination to escalate load bearing on the pedicle screw-rod construct, with a value of 87.1 MPa. This was followed by the bilateral titanium (69.1 MPa), obliquely-placed PEEK (68.5 MPa), and bilateral PEEK (61.7 MPa) cages. It is worth noting that the double spacer configuration demonstrated improved load distribution on the bone-pedicle screw junctions regardless of the cage material. However, if only the material is considered, higher stress profiles were observed on the stiffer material (titanium), irrespective of the number of spacers and cage configurations.

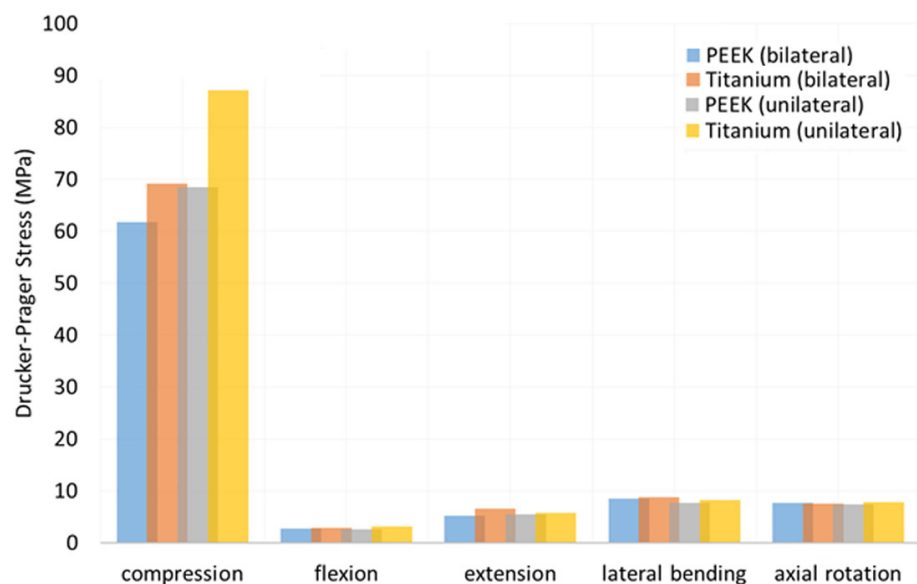


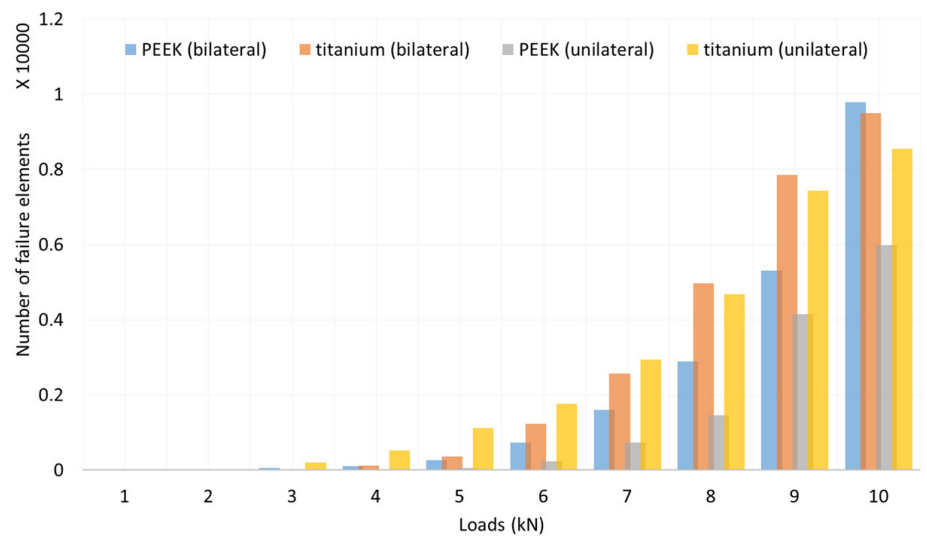
Fig. 8. Bone-pedicle screw interface stress

Relative stress concentration gap difference. The study employed the relative stress concentration gap difference between the cage-endplate and bone-pedicle screw interface to assess the stress mitigation effect on the cage-endplate junction. The computed relative stress concentration differences for the unilateral PEEK, bilateral PEEK, bilateral titanium, and unilateral titanium cage constructs were found to be 73%, 67%, 65%, and 57%, respectively. These findings showed that the PEEK-based cage effectively reduces the load dispersal on the frontal part of the spine. Additionally, the obliquely-placed cage construct was particularly effective in mitigating interface stress at the cage-endplate. The higher magnitude of the relative stress concentration gap indicates that a significant portion of the load is transferred through the pedicle screw-rod construct. This reduces stress at the cage-endplate interface, ultimately decreasing the incidence of cage sinking.

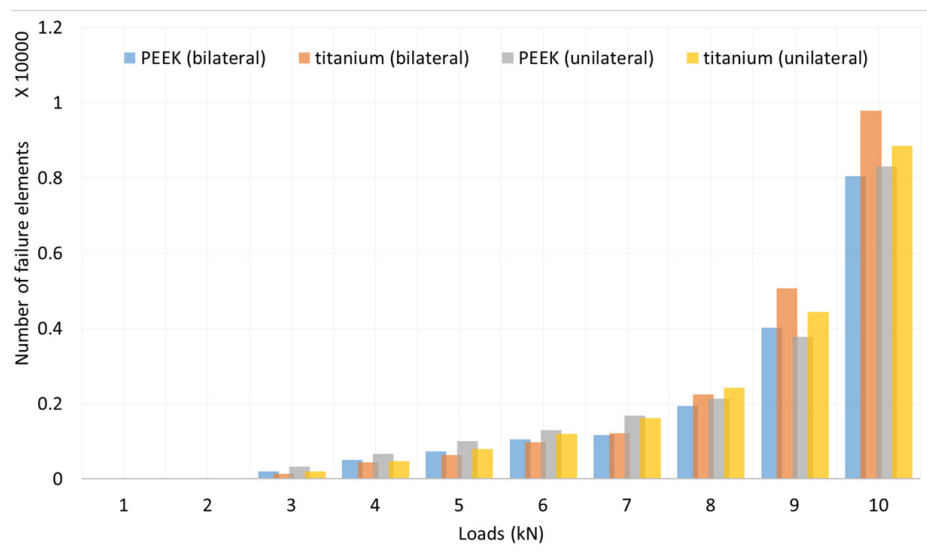
3.2 Failure element distributions

Figure 9 shows the chronological changes of the failure element distributions under incrementally increasing loads of 1 to 10 kN to replicate the high-impact loading condition. These two graphs describe the effects of cage subsidence and the

screw loosening symptom. The respective graphical representations of the yielding and failure elements under 8 kN loads are shown in Figure 10. The findings indicate that the PEEK-based cage construct had the least deformed elements. The obliquely-placed unilateral PEEK cage could significantly reduce cage subsidence effects, but at the same time, it would slightly increase the loosening effect on the bone–pedicle screw junction. However, for the bilateral PEEK cage, the response was reciprocal. Thus, the obliquely-placed unilateral cage construct was shown to be the best clinical approach since reducing the impact of cage subsidence is significantly more advantageous than reducing the effects of pedicle screw loosening. This is based on the relative difference of the deformed elements between the two cage constructs at the bone–pedicle screw and cage–endplate junctions, which was 39% and 3% (readings at 10 kN), respectively. In addition, the onset fracture load for this construct was 6 kN, considered the toughest PLIF construct.



Subsidence effects



Loosening effects

Fig. 9. Historical changes of failure element distribution

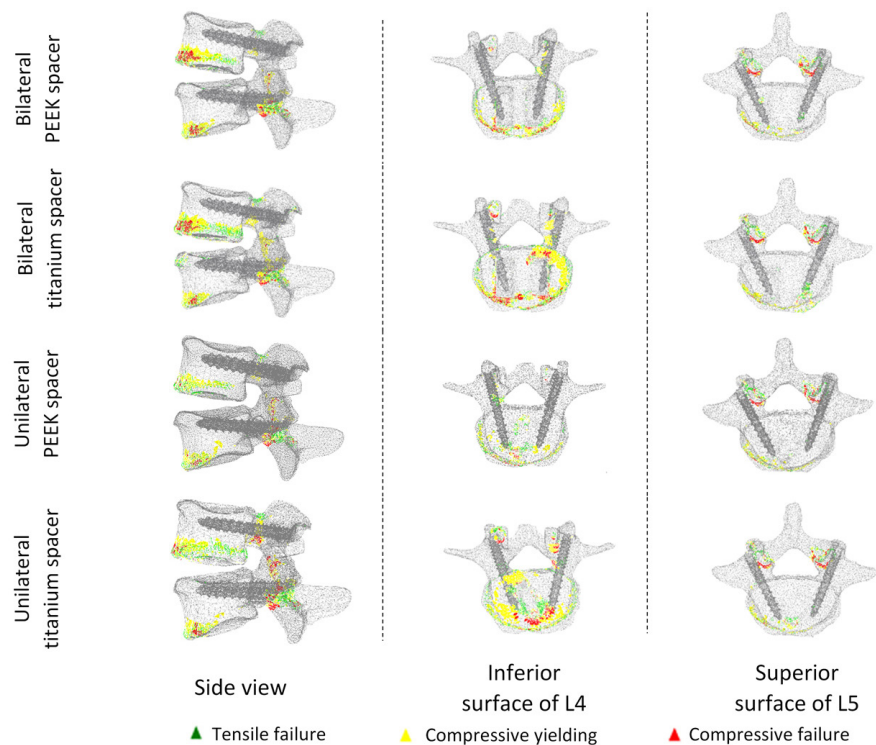


Fig. 10. Graphical representation of failure element distribution under the application of 8 kN compressive load

As for the titanium-based cage, the PLIF construct acted differently in low to middle (1 to 8 kN) and high (9–10 kN) input loads. The bilateral cage configuration showed fewer failure elements in the low to middle input loads than the unilateral cage configuration at cage-endplates and pedicle screw-bone interfaces. On the contrary, they acted the opposite at the high input loads, with higher numbers of failure elements generated by the bilateral cage configuration in both adjoining areas. This condition might be related to a more severe screw-loosening effect on the bilateral cage configuration based on the high accumulation of failure elements on the bone-pedicle screw junction. This, in tandem, increased the stress on the cage-endplate junction by allowing large amounts of loads to transmit through the stiff cage material to cause further deterioration on their surface areas. Based on the considerations above, we assumed that the obliquely-placed unilateral titanium cage construct is the most unreliable PLIF construct because it tends to cause a higher risk of bone fracturing, even under the impact of a non-traumatic event.

3.3 Spine ROM

The ROM for the simulated fusion constructs is shown in Figure 11. The minimal ROM for compression, flexion, extension, lateral bending and axial rotation could be detected with bilateral titanium, bilateral PEEK, unilateral PEEK, and unilateral PEEK and bilateral titanium fusion constructs, respectively. The unilateral PEEK and the bilateral titanium fusion constructs exhibited more activities that produced the most minimal ROM. However, the bilateral titanium fusion construct showed the greatest ROM under flexion and lateral bending motions. The accumulated ROM for each activity can be summarized as follows (from the greatest to the lowest): bilateral

PEEK (56.9°), bilateral titanium (54.1°), unilateral titanium (51.2°), and unilateral PEEK (49.5°) cage constructs. We assumed that the most stable PLIF construct must be the reconstructive structure with the highest frequency of minimal stress generations and produced the smallest accumulative ROM. Based on these criteria, we concluded that the obliquely-placed PEEK is the most stable PLIF cage construct compared to others. From the mechanical viewpoint, stability is the most important criterion in determining the lifespan of the reconstructive reconfiguration before a revision surgery is required to rectify any spinal health-related issues.

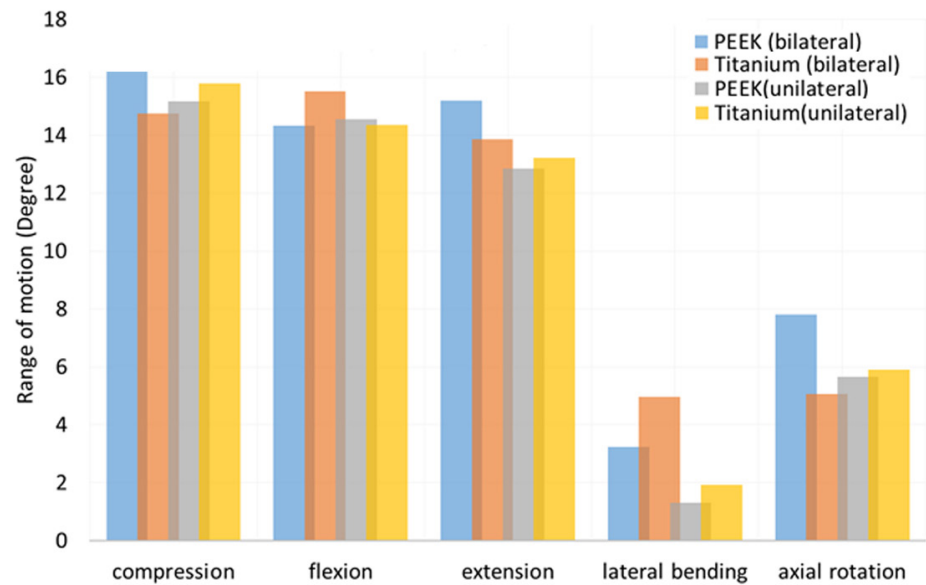


Fig. 11. Vertebral range of motion

4 DISCUSSION

The biomechanical advantages of PEEK over titanium have been extensively discussed in spinal surgery, primarily due to its lower modulus of elasticity (MOE) that closely matches cortical bone [3–7]. The study's findings demonstrate that using PEEK material can significantly lessen the stress shielding effect and improve load sharing. This was evident in the lower stress levels observed in PEEK constructs compared to titanium spacers at both the end-plate and facet joint junctions. Importantly, almost all maximal interface stresses remained below the average yield strength of normal bone (83 MPa) [22]. The exception was the bone-pedicle screw junction in the case of the obliquely-placed titanium cage, suggesting a higher incidence of fracture (screw loosening effect) in the unilateral titanium cage construct. However, it should be noted that the study did not consider the dynamic factor, which is typically five times higher than the static state [23]. Therefore, the margin of safety for most reconstructive configurations may not be satisfactory and could be susceptible to bone fracturing. Future research should incorporate the dynamic factor to validate these findings further.

The analysis of stress profiles aligns well with the assessment of fracture risks, highlighting the higher likelihood of cage subsidence and pedicle screw loosening in titanium-based cage constructs. This is evidenced by the presence of a larger number of failure elements in those areas and fractures at lower loads. Based on these findings, it is concluded that titanium-based spacers are not recommended for patients with osteoporosis. This is because osteoporosis exacerbates the stress

shielding effect, compromising the structural integrity of the reconstructive configuration and increasing the risk of bone fractures even during basic daily activities. An FEA study by Adam et al. [2] demonstrated that severe osteoporosis in a vertebral body model resulted in endplate stress levels up to three times higher than in a healthy bone. Therefore, the notable characteristics of PEEK, such as low stiffness and high ultimate and tensile strengths [6], make it highly applicable and biocompatible for use as a cage material in PLIF surgery.

The lower stress in PEEK spacers leads to reduced subsidence of the spacers into the endplate. This can be attributed to the effective transfer of higher stress through the rigid structure of the rod and pedicle screw system. This aligns with the objective of using PI to offer structural support to the spine [14]. The point of attachment between the vertebral body and the screw plays a crucial role in supporting and transferring loads effectively. It has been reported that PI can significantly reduce the stress at the cage-endplate interface by 50–60% compared to non-instrumented cages [1]. Furthermore, PI can also alleviate the possibilities of cage failure and migration by aggregating the resistance to cage pullout [9,11]. Although it may seem that increased stress on the pedicle screw could impose a higher load burden on that area, it is important to note that the stress generated by PEEK-based cage constructs is generally lower than titanium-based cage constructs. As mentioned earlier, the biomechanical superiority of PEEK-based constructs over titanium-based ones has been discussed. Therefore, in the subsequent explanations, we will not discuss any effects associated with titanium-based cage constructs.

Adopting a single cage configuration has become a viable alternative and the center of much attention ever since PI has become feasible as a load-supporting structure, thus surpassing the need to implant a bilateral cage configuration [1,8,9,11]. This is because, according to Tsuang et al. [1], a standalone bilateral cage insertion could, at best, only reduce the stress generation at the cage-endplate interface by 33%. Moreover, most experiments have shown that applying a bilateral cage would increase the risk of spinal injuries and incur higher costs [8]. Dural tears, kyphosis and severe back pain are PLIF-related diseases that could confine an individual's mobility and thus lessen their quality of life. Based on this notion, we assume that by instrumenting PI, adding a second cage will become redundant and less effective. Furthermore, reducing cage-endplate stress might be related to a smaller cage area in contact with an endplate than bilateral cage insertions. The rule of thumb is that a small contact surface area will damage the surrounding structures, while a large contact surface area will reduce implant stability. In this study, we have found that the application of unilateral cage insertion in PEEK-based cage constructs has achieved the most excellent stress reduction in both cage-endplate and bone pedicle screw interfaces. As a result, the effects of cage subsidence and pedicle screw loosening were also significantly reduced. Furthermore, this reconstructive configuration could be easily adapted to normal and traumatic events.

Based on our findings, the obliquely-placed unilateral PEEK cage construct was conclusively regarded as the most stable PLIF by offering structural symmetry to the construct. Theoretically, even though the optimization of the structural symmetry could only be achieved by placing the cage sagittally in the midline, this configuration requires too invasive an incision, exposing the nerve root to damage. The mechanical stability of the model was dictated by minimal spine ROM. The results obtained in this study are consistent with the preceding findings conducted by Cho et al. [24], Tsuang et al. [1], and Chiang et al. [11] using an FEA approach. In the reports, most of them agreed that the implementation of obliquely-placed single PLIF cages with PI showed biomechanical stability on par with bilateral PLIF cage construct. They also reported that this construct could generate less stress on the

cage-endplate junction and, to some extent, increase the stress on the facet joints compared to double cage fusion. Our results also suggest that instability is the underlying cause of the increased screw loosening effect. This is because inadequate stabilization might increase micro-motion movability, elevate the pedicle screw and rod system stress, and finally accelerate the screw loosening [9]. Finally, it is also important to note that PI is the main contributor to maintaining the postoperative stability of the PLIF construct. It has been reported that instrumenting PI could significantly reduce the ROM at the index level by between 80% and 99% compared to an intact condition [25]. Therefore, integrating an oblique configuration in conjunction with PI would result in the best clinical outcomes.

5 CONCLUSIONS

The choice of cage material and the cage configuration's orientation are key factors in achieving better mechanical and clinical outcomes in PLIF surgery. The use of an obliquely-placed unilateral PEEK spacer with posterior instrumentation (PI) offers several advantages, including immediate stability, reduced cage subsidence, and decreased risk of pedicle screw loosening. This surgical technique has the potential to be an alternative to bilateral cage fusions, as it can lower surgical costs and minimize the risks of construct failure and spinal injuries. However, further analysis and clinical experimentation are needed to refine the applicability of this reconstructive configuration. It's important to note that this paper has limitations as it has yet to be experimentally validated. The results presented are based on relative comparisons among various fusion cage constructs, highlighting the significant factors for consideration in this and future studies. Future research could focus on further developing cage materials and designs to achieve an optimized biomechanical construct. One promising option is the introduction of new PEEK/titanium-based composites combined with flexible fixation using PI. However, such options need to be validated through experimental and virtual studies to assess their effectiveness and safety.

6 ACKNOWLEDGEMENT

This research was supported by the Ministry of Higher Education (MOHE) through the Fundamental Research Grant Scheme for Research Acculturation of Early Career Researchers (RACER 1/2019/TK03/UTHM//1). We also want to thank Universiti Tun Hussein Onn Malaysia and the UTHM Publisher's Office, which provides monetary assistance that makes the communication of this research possible via Publication Fund E15216 and the GPPS (vot Q287).

7 REFERENCES

- [1] Y. H. Tsuang, Y. F. Chiang, C. Y. Hung, H. W. Wei, C. H. Huang, and C. K. Cheng, "Comparison of cage application modality in posterior lumbar interbody fusion with posterior instrumentation – A finite element study," *Medical Engineering & Physics*, vol. 31, no. 5, pp. 565–570, 2009. <https://doi.org/10.1016/j.medengphy.2008.11.012>
- [2] C. Adam, M. Pearcy, and P. M. Combe, "Stress analysis of interbody fusion-finite element modelling of intervertebral implant and vertebral body," *Clinical Biomechanics*, vol. 18, no. 4, pp. 265–272, 2003. [https://doi.org/10.1016/S0268-0033\(03\)00022-6](https://doi.org/10.1016/S0268-0033(03)00022-6)

- [3] S. M. Kurtz and J. N. Devine, "PEEK biomaterials in trauma, orthopedic, and spinal implants," *Biomaterials*, vol. 28, no. 32, pp. 4845–4869, 2007. <https://doi.org/10.1016/j.biomaterials.2007.07.013>
- [4] R. J. Mobbs, A. M. Chau, and D. Durmush, "Biphasic calcium phosphate contains within polyetheretherketone cage with and without plating for anterior cervical discectomy and fusion," *Orthopedic Surgery*, vol. 4, no. 3, pp. 156–165, 2012. <https://doi.org/10.1111/j.1757-7861.2012.00185.x>
- [5] M. Cabraja, S. Oezdemir, D. Koeppen, and S. Kroppenstedt, "Anterior cervical discectomy and fusion: Comparison of titanium and polyetheretherketone cages," *BMC Musculoskeletal Disorder*, vol. 13, p. 172, 2012. <https://doi.org/10.1186/1471-2474-13-172>
- [6] C. C. Niu, J. C. Liao, W. J. Chen, and L. H. Chen, "Outcomes of interbody fusion cages used in 1 and 2-levels anterior cervical discectomy and fusion: Titanium cages versus polyetheretherketone (PEEK) cages," *Journal of Spinal Disorders & Techniques*, vol. 23, no. 5, pp. 310–316, 2010. <https://doi.org/10.1097/BSD.0b013e3181af3a84>
- [7] E. Chong, M. H. Pelletier, R. J. Mobbs, and W. R. Walsh, "The design evolution of interbody cages in anterior cervical discectomy and fusion," *BMC Musculoskeletal Disorder*, vol. 16, p. 99, 2015. <https://doi.org/10.1186/s12891-015-0546-x>
- [8] R. W. Monilari, J. Sloboda, and F. L. Johnstone, "Are two cages needed with instrumented PLIF? A comparison of 1 versus 2 interbody cages in a military population," *The American Journal of Orthopedics*, vol. 32, pp. 337–343, 2003.
- [9] D. V. Ambati, E. K. Wright, R. A. Lehman, D. G. Kang, S. C. Wagner, and A. E. Dmitriev, "Bilateral pedicle screw fixation provides biomechanical stability in transforaminal lumbar interbody fusion: A finite element study," *The Spine Journal*, vol. 15, no. 8, pp. 1812–1822, 2015. <https://doi.org/10.1016/j.spinee.2014.06.015>
- [10] S. T. Wang, V. K. Goel, C. Y. Fu, S. Kubo, W. Choi, C. L. Liu, *et al.*, "Posterior instrumentation reduces differences in spine stability as a result of different cage orientations: An in vitro study," *Spine*, vol. 30, no. 1, pp. 62–67, 2005. <https://doi.org/10.1097/01.brs.0000150123.26869.48>
- [11] M. F. Chiang, Z. C. Zhong, C. S. Chen, C. K. Cheng, and S. L. Shih, "Biomechanical comparison of instrumented posterior lumbar interbody fusion with one or two cages by finite element analysis," *Spine*, vol. 31, no. 19, pp. 682–689, 2006. <https://doi.org/10.1097/01.brs.0000232714.72699.8e>
- [12] J. H. Keyak, S. A. Rossi, K. A. Jones, and H. B. Skinner, "Prediction of femoral fracture load using automated finite element modeling," *Journal of Biomechanics*, vol. 31, no. 2, pp. 125–133, 1998. [https://doi.org/10.1016/S0021-9290\(97\)00123-1](https://doi.org/10.1016/S0021-9290(97)00123-1)
- [13] M. Alizadeh, M. R. Kadir, M. M. Fadhli, A. Fallahiarezoodar, B. Azmi, M. R. Murali, and T. Kamarul, "The use of x-shaped cross-link in posterior spinal constructs improves stability in thoracolumbar burst fracture: A finite element analysis," *Journal of Orthopaedic Research*, vol. 31, no. 9, pp. 1447–1454, 2013. <https://doi.org/10.1002/jor.22376>
- [14] D. Tawara, K. Noro, T. Tsujikami, Y. Okamoto, and H. Murakami, "Nonlinear mechanical analysis of posterior spinal instrumentation for osteoporotic vertebra: Effects of mechanical properties of the rod on the failure risks around the screw," *Journal of Biomechanical Science and Engineering*, vol. 9, no. 2 S1, pp. 13–163, 2014. <https://doi.org/10.1299/jbse.13-00163>
- [15] K. S. Han, A. Rohlmann, T. Zander, and W. R. Taylor, "Lumbar spinal loads vary with body height and weight," *Medical Engineering and Physics*, vol. 35, no. 7, pp. 969–977, 2013. <https://doi.org/10.1016/j.medengphy.2012.09.009>
- [16] L. Zhang, G. Yang, L. Wu, and B. Yu, "The biomechanical effects of osteoporosis vertebral augmentation with cancellous bone granules or bone cement on treated and non-treated vertebral bodies: A finite element evaluation," *Clinical Biomechanics*, vol. 25, no. 2, pp. 166–172, 2010. <https://doi.org/10.1016/j.clinbiomech.2009.10.006>

- [17] O. Perey, "Fracture of the vertebral endplate in the lumbar spine," *Acta Orthop Scand*, vol. 25, pp. 34–39, 1957.
- [18] C. R. Dale' Bass, K. A. Rafaels, R. S. Salzar, S. Carboni, R. W. Kent, M. D. Lloyd, S. Lucas, K. Meyerhoff, C. Planchak, A. Damon, and G. T. Bass, "Thoracic and lumbar spinal impact tolerance," *Accident Analysis and Prevention*, vol. 40, no. 2, pp. 487–495, 2008. <https://doi.org/10.1016/j.aap.2007.08.006>
- [19] T. S. Kaneko, M. R. Pejcic, J. Tehranzadeh, and J. H. Keyak, "Relationships between material properties and CT scan data of cortical bone with and without metastatic lesions," *Medical Engineering Physics*, vol. 25, no. 6, pp. 445–454, 2003. [https://doi.org/10.1016/S1350-4533\(03\)00030-4](https://doi.org/10.1016/S1350-4533(03)00030-4)
- [20] M. Bessho, I. Ohnishi, J. Matsuyama, T. Matsumoto, K. Imai, and K. Nakamura, "Prediction of strength and strain of the proximal femur by a CT-based finite element method," *Journal of Biomechanics*, vol. 40, no. 8, pp. 1745–1753, 2007. <https://doi.org/10.1016/j.jbiomech.2006.08.003>
- [21] E. Ibarz, A. Herrera, Y. Mas, J. Rodriguez-Vela, J. Cegonino, S. Puertolas, and L. Gracia, "Development and kinematic verification of a finite element model for the lumbar spine: Application to disc degeneration," *Biomed Research International*, 2013. <https://doi.org/10.1155/2013/705185>
- [22] F. G. Evans, *Mechanical Properties of Bone*. Springfield, IL: Charles C Thomas, 1973.
- [23] Y. Okamoto, H. Murakami, S. Demura, S. Kato, K. Yoshioka, H. Hayashi, J. Sakamoto, N. Kawahara, and H. Tsuchiya, "The effect of kyphotic deformity because of vertebral fracture: A finite element analysis of a 10° and 20° wedge-shaped vertebral fracture model," *The Spine Journal*, vol. 15, no. 4, pp. 713–720, 2015. <https://doi.org/10.1016/j.spinee.2014.11.019>
- [24] W. Cho, C. Wu, A. A. Mehbobb, and E. E. Transfedt, "Comparison of cage designs for transforminal lumbar interbody fusion: A biomechanical study," *Clinical Biomechanics*, vol. 23, no. 8, pp. 979–985, 2008. <https://doi.org/10.1016/j.clinbiomech.2008.02.008>
- [25] W. F. Beringer and J. P. Mobasser, "Unilateral pedicle screw implementation for minimally invasive transforminal lumbar interbody fusion," *Neurosurgical Focus*, vol. 20, no. 3, pp. 1–5, 2006. <https://doi.org/10.3171/foc.2006.20.3.5>

8 AUTHORS

Nur Saliha Md Salleh is a master's student at the Faculty of Electrical and Electronic Engineering, Universiti Tun Hussein Onn Malaysia, 86400 Parit Raja, Johor, Malaysia (E-mail: ge200067@student.uthm.edu.my).

Muhammad Hazli Mazlan is a Senior Lecturer and Principle Researcher at the Faculty of Electrical and Electronic Engineering, Universiti Tun Hussein Onn Malaysia. He is currently working in biomedical engineering research areas specializing in orthopedic implants and image processing analysis (E-mail: mhazli@uthm.edu.my).

Muhammad Anas Razali is a Senior Lecturer and Head of Research Focus Group at the Faculty of Electrical and Electronic Engineering, Universiti Tun Hussein Onn Malaysia. He is currently working in biomedical and microelectronic research areas (E-mail: anas@uthm.edu.my).